

See discussions, stats, and author profiles for this publication at: <https://www.researchgate.net/publication/5331461>

Head-to-Head (HH) and Head-to-Tail (HT) Conformers of cis-Bis Guanine Ligands Bound to the $[\text{Re}(\text{CO})_3]^+$ Core

ARTICLE *in* INORGANIC CHEMISTRY · APRIL 2004

Impact Factor: 4.76 · DOI: 10.1021/ic035012a · Source: PubMed

CITATIONS

31

READS

42

5 AUTHORS, INCLUDING:



Fabio Zobi

Université de Fribourg

74 PUBLICATIONS 501 CITATIONS

SEE PROFILE



Olivier Blacque

University of Zurich

187 PUBLICATIONS 2,406 CITATIONS

SEE PROFILE



Helmut W. Schmalle

University of Zurich

220 PUBLICATIONS 4,596 CITATIONS

SEE PROFILE

Head-to-Head (HH) and Head-to-Tail (HT) Conformers of *cis*-Bis Guanine Ligands Bound to the $[\text{Re}(\text{CO})_3]^+$ CoreFabio Zobi,[†] Olivier Blacque, Helmut W. Schmalle, Bernhard Spingler, and Roger Alberto*Institute of Inorganic Chemistry, University of Zürich, Winterthurerstrasse 190,
CH-8057 Zürich, Switzerland

Received August 28, 2003

We have prepared four complexes of the type $[\text{Re}(\text{guanine})_2(\text{X})(\text{CO})_3]$ (guanine = 9-methylguanine or 7-methylguanine, X = H_2O or Br) in order to understand the factors determining the orientation of coordinated purine ligands around the $[\text{Re}(\text{CO})_3]^+$ core. The 9-methylguanine ligand (9-MeG) was chosen as the simplest N(9) derivatized guanine, and 7-methylguanine (7-MeG) was chosen because metal binding to N(9) does not impose steric hindrance. Two types of structures have been elucidated by X-ray crystallography, an HH (head-to-head) and HT (head-to-tail) conformer for each of the guanines. All complexes crystallize in monoclinic space groups: $[\text{Re}(9\text{-MeG})_2(\text{H}_2\text{O})(\text{CO})_3]\text{ClO}_4$ (**2**) in $P2_1/n$ with $a = 12.3307(10)$ Å, $b = 16.2620(14)$ Å, $c = 13.7171(11)$ Å, and $\beta = 105.525(9)^\circ$, $V = 2650.2(4)$ Å³, with the two bases in HT orientation and its conformer $[\text{Re}(9\text{-MeG})_2(\text{H}_2\text{O})(\text{CO})_3]\text{Br}$ (**3**) in $P2_1/n$ with $a = 15.626(13)$ Å, $b = 9.5269(5)$ Å, $c = 15.4078(13)$ Å, and $\beta = 76.951(1)^\circ$, $V = 2234.5(3)$ Å³, and the two bases in an HH orientation. Similarly, $[\text{Re}(7\text{-MeG})_2(\text{H}_2\text{O})(\text{CO})_3]\text{ClO}_4$ (**4**) crystallizes in $P2_1/c$ with $a = 13.0708(9)$ Å, $b = 15.4082(7)$ Å, $c = 14.316(9)$ Å, and $\beta = 117.236(7)^\circ$, $V = 2563.5(3)$ Å³, and exhibits an HT orientation and $[\text{ReBr}(7\text{-MeG})_2(\text{CO})_3]$ (**5**) in $P2_1/c$ with $a = 17.5117(9)$ Å, $b = 9.8842(7)$ Å, $c = 15.3539(1)$ Å, and $\beta = 100.824(7)^\circ$, $V = 2610.3(3)$ Å³, and shows an HH orientation. When crystals of any of these complex pairs are dissolved in D_2O , the ^1H NMR spectrum shows a single peak for the H(8) resonance of the respective coordinated purine indicating a rapid equilibrium between HH and HT conformations in solution. DFT calculations simulating the rotation of one ligand around its Re–N bond showed energetic barriers of less than 8.7 kcal/mol. We find no hypochromic effect in the Raman spectrum of **3**, which showed base stacking in the solid state. Neither steric interactions nor hydrogen bonding are important in determining the orientation of the ligands in the coordination sphere.

Introduction

It is now generally accepted that the cytotoxicity of the anticancer drug cisplatin is due to the formation of 1,2-intrastrand adducts between the N7 atoms of two adjacent guanine residues in DNA.¹ Early structure–activity relationship studies indicated that for any *cis*-PtA₂X₂ analogue of cisplatin (A₂ is two amines or a bidentate amine ligand and X is an anionic leaving group) the carrier amine ligand had to have at least one proton for the drug to retain its anticancer

activity.² This observation, along with the realization that d(GpG) can assume different conformations around the metal core,³ led to the hypothesis that hydrogen bonding interactions between bound G ligands and the carrier amine of the drug were important for the stabilization of the DNA distortion induced by the intrastrand lesion.^{3a,4}

By using the so-called “retro models”, Marzilli, Natile, and their co-workers have later demonstrated that the guanine O6 H-bonding to carrier amine ligand hydrogen is not important for the bases to assume a particular orientation

* To whom correspondence should be addressed. E-mail: ariel@aci.unizh.ch.

[†] E-mail: fabio@aci.unizh.ch.

- (1) (a) Jamieson, E. R.; Lippard, S. J. *Chem. Rev.* **1999**, *99*, 2467–2498. (b) Spingler, B.; Whittington, D. A.; Lippard, S. J. *Inorg. Chem.* **2001**, *40*, 5596–5602. (c) Takahara, P. M.; Frederick, C. A.; Lippard, S. J. *J. Am. Chem. Soc.* **1996**, *118*, 12309–12321. (d) Gelasco, A.; Lippard, S. J. *Biochemistry* **1998**, *37*, 9230–9239.

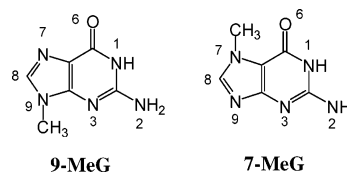
- (2) Wong, H. C.; Intini, F. P.; Natile, G.; Marzilli, L. G. *Inorg. Chem.* **1999**, *38*, 1006–1014.

- (3) (a) Xu, Y.; Natile, G.; Intini, F. P.; Marzilli, L. G. *J. Am. Chem. Soc.* **1990**, *112*, 8177–8179. (b) Ano, S. O.; Intini, F. P.; Natile, G.; Marzilli, L. G. *J. Am. Chem. Soc.* **1997**, *119*, 8570–8571. (c) Ano, S. O.; Intini, F. P.; Natile, G.; Marzilli, L. G. *J. Am. Chem. Soc.* **1998**, *120*, 12017–12022. (d) Marzilli, L. G.; Ano, S. O.; Intini, F. P.; Natile, G. *J. Am. Chem. Soc.* **1999**, *121*, 9133–9142.

around the metal center, and they hypothesized that the small size of the NH group rather than its hydrogen-bonding ability is important for the anticancer activity of the drug.⁵ In the area of new drug design, much interest remains in understanding the factors driving the formation of different head-to-head (HH) and head-to-tail (HT) conformers of the *cis*-PtA₂{d(GpG)} complex. One principal hypothesis, originally advanced by Lippard to explain the activity of the drug, suggests that the HH form in the intrastrand lesion is recognized by a damage recognition protein whose binding prevents DNA repair, allowing the cisplatin adduct to persist long enough to activate apoptosis.⁶ Marzilli suggested that the HT form in the interstrand lesion causes weaker binding of the damage recognition protein making this lesion a better substrate for repair.⁷ Therefore, according to this hypothesis, the formation of an HT conformer results in lower cytotoxicity of the drug.

While our current interest remains the development of [M(CO)₃]⁺-based chemo- and radiopharmaceuticals (M = Re, ^{99m}Tc), it is within the above-mentioned context that this work is presented. Rhenium tricarbonyl complexes have been reported to suppress the growth of tumor cell lines, via coordination to N7 in guanine bases in a fashion similar to cisplatin, and this event was anticipated to be a possible mode of action for some of these Re complexes.⁸ We have recently shown that the [M(CO)₃]⁺ core (M = Re, ⁹⁹Tc) can bind two guanine bases in a *cis* fashion, and we have shown by X-ray crystallography that the two bases are in an HT conformation around the Re metal core.⁹ Tailoring new DNA-targeting chemotoxic agents based on a metal or metal fragment of octahedral geometry, which results exclusively in the formation of an HT conformer when bound to two purine bases, might be expected, for the reasons mentioned above, as being of low efficacy. Reedijk and others have pointed out that the carbonyl oxygen of coordinated guanine becomes sterically demanding in octahedral complexes; therefore, steric hindrance between O(6) in 9-MeG and the CO ligands might explain the preferred HT form we found in the case of the rhenium tricarbonyl complex.¹⁰

Chart 1. Structure of 9-MeG and 7-MeG with Numbering of Relevant Atoms



In order to understand the factors determining the orientation of purine bases when coordinated to the [Re(CO)₃]⁺ core, and more generally to a metal of octahedral geometry, we have studied the interaction of [Re(H₂O)₃(CO)₃]⁺ with 9-methylguanine (9-MeG) and 7-methylguanine (7-MeG) (Chart 1). The first of the two ligands was chosen as the simplest N(9) derivatized guanine, while 7-MeG was chosen because metal binding to N(9) does not impose steric hindrance. Here we present, for the first time, structural evidence that, as in the Pt case, two guanine ligands can adopt several conformations in an octahedral [(CO)₃Re-(purine)₂X] complex (X = H₂O, Br). Our results suggest that neither hydrogen bonding interactions nor steric factors are important in determining the orientation of the ligands. The apparent intramolecular hydrogen bonding interactions one observes in the solid state structures result from the intrinsic conformation assumed by the ligands when bound to [Re(CO)₃]⁺ core. The presence of HH and HT conformers in complexes with either 9-MeG or 7-MeG points to the fact that the steric hindrance imposed by the carbonyl oxygen of coordinated guanine is not a driving force for the preference of one conformation over the other.

Experimental Section

Materials. All reagents and solvents were used as received. Methanol and dichloromethane were purchased from Merck, and all other solvents and reagents were obtained from Fluka. The complex [Et₄N]₂[ReBr₃(CO)₃] (**1**) was prepared according to the reported procedures.¹¹ HPLC chromatograms were measured on a Merck Hitachi LaChrom D-7000 instrument. HPLC system, RP-18 column (A = 0.1% CF₃COOH in H₂O, B = MeOH): 0–3 min 100% A; 3–9 min 75% A; 9.1 min 66% A; 9.1–20 min 66% → 0% A; 20–25 min 0% A; 25.1–30 min 100% A.

IR and Raman Spectroscopy. Infrared spectra were recorded on a Perkin-Elmer BX II spectrometer from KBr pellets. Raman spectra were taken on a Remishaw Ramanscope with He–Ne laser excitation (633 nm). Wavenumber calibration was obtained by means of Si (100); scan rates were usually 10 cm^{−1} min^{−1}.

NMR Spectroscopy. All NMR samples were prepared in D₂O by dissolving crystals of the desired complex (typically 1–1.5 mM) and immediately transferring the samples to the probe. All ¹H NMR 1D spectra were recorded on a Bruker 500 MHz spectrometer. The residual HOD peak was used as reference.

[Re(9-MeG)₂(H₂O)(CO)₃]ClO₄·3H₂O (**2**). A 30 mg (0.04 mmol) portion of **1** was dissolved in hot (~40 °C) methanol (3 mL), and 28 mg (0.14 mmol) of AgClO₄ was added. The solution was stirred for 3 h; AgBr was filtered off. A 16.5 mg (0.1 mmol) portion of

- (4) (a) Hambley, T. W. *Inorg. Chem.* **1991**, *30*, 937–942. (b) Vickery, K.; Bonin, A. M.; Fenton, R. R.; O'Mara, S.; Russell, P. J.; Webster, L. K.; Hambley, T. W. *J. Med. Chem.* **1993**, *36*, 3663–3668. (c) Fenton, R. R.; Easdale, W. J.; Er, H. M.; O'Mara, S. M.; McKeage, M. J.; Russell, P. J.; Hambley, T. W. *J. Med. Chem.* **1997**, *40*, 1090–1098. (d) Rezler, E. M.; Fenton, R. R.; Easdale, W. J.; McKeage, M. J.; Russell, P. J.; Hambley, T. W. *J. Med. Chem.* **1997**, *40*, 3508–3515. (e) Hambley, T. W. *Coord. Chem. Rev.* **1997**, *166*, 181–223. (f) Guo, Z.; Sadler, P. J.; Zang, E. *J. Chem. Soc., Chem. Commun.* **1997**, 27–28.
- (5) (a) Sullivan, S. T.; Ciccacese, A.; Fanizzi, F. P.; Marzilli, L. G. *J. Am. Chem. Soc.* **2001**, *123*, 9345–9355. (b) Williams, K. M.; Scarcia, T.; Natile, G.; Marzilli, L. G. *Inorg. Chem.* **2001**, *40*, 445–454. (c) Saad, J. S.; Scarcia, T.; Natile, G.; Marzilli, L. G. *Inorg. Chem.* **2002**, *41*, 4923–4935.
- (6) Pil, P.; Lippard, S. J. *Science* **1992**, *256*, 234–237.
- (7) Sullivan, S. T.; Ciccacese, A.; Fanizzi, F. P.; Marzilli, L. G. *Inorg. Chem.* **2000**, *39*, 836–842.
- (8) (a) Yan, Y.-K.; Cho, S. E.; Shaffer, K. A.; Rowell, J. E.; Barnes, B. J.; Hall, I. H. *Pharmazie* **2000**, *55*, 307–313. (b) Zhang, J.; Vittal, J. J.; Henderson, W.; Wheaton, J. R.; Hall, I. H.; Hor, T. S. A. Yan, Y.-K. *J. Organomet. Chem.* **2002**, *650*, 123–132.
- (9) Zobi, F.; Spingler, B.; Fox, T.; Alberto, R. *Inorg. Chem.* **2003**, *42*, 2818–2820.
- (10) Van Vliet, P. M.; Haasnoot, J. G.; Reedijk, J. *Inorg. Chem.* **1994**, *33*, 1934–1939.

- (11) (a) Alberto, R.; Egli, A.; Abram, U.; Hegetschweiler, K.; Gramlich, V.; Schubiger, P. A. *J. Chem. Soc., Dalton Trans.* **1994**, *19*, 2815–2820. (b) Alberto, R.; Schibler, R.; Egli, A.; Schubiger, P. A.; Herrmann, W. A.; Artus, G.; Abram, U.; Kaden, T. A. *J. Organomet. Chem.* **1995**, *493*, 119–127.

9-MeG were added, and the mixture was heated to 50 °C under a slight N₂ pressure. The colorless solution turned light yellow within minutes. The reaction was monitored by HPLC and was stopped after 3.5 h when no further change could be observed. The solution was allowed to come to room temperature, concentrated, and purified on a short C18 column. To the methanol fraction containing the purified complex was added 3% H₂O (v/v). Pentane was allowed to diffuse into the solution depositing X-ray quality crystals. Yield: quantitative. Anal. Calcd: C% 25.1, N% 19.5, H% 2.3. Found: C% 25.8, N% 19.0, H% 2.7. ¹H NMR data (in D₂O, δ, ppm): H8 8.09, CH₃ 3.69. IR data (KBr pellet, ν, cm⁻¹): CO 2027 (s), 1918 (b), 1897 (b). MS data ESI+: 600.3 *m/z* = ([M]⁺ - H₂O).

[Re(9-MeG)₂(H₂O)(CO)₃]Br·H₂O (3). To 30 mg (0.04 mmol) of **1** in water (5 mL) was added 16.5 mg (0.1 mmol) of 9-MeG, and the mixture was heated to 50 °C under a slight N₂ pressure. After 3.5 h, the reaction was stopped, allowed to come to room temperature, concentrated, and purified on a short C18 column. The methanol fraction containing the purified complex was concentrated to about 1 mL, and then, 4 mL of water was added. Slow solvent evaporation deposited X-ray quality crystals of **3** after one week. Yield: quantitative. Anal. Calcd: C% 25.2, N% 19.6, H% 2.5. Found: C% 25.3, N% 19.5, H% 2.8. ¹H NMR data (in D₂O, δ, ppm): H8 8.09, CH₃ 3.69. IR data (KBr pellet, ν, cm⁻¹): CO 2027 (s), 1915 (b), 1895 (b). MS data ESI+: 600.3 *m/z* = ([M]⁺ - H₂O).

[Re(7-MeG)₂(H₂O)(CO)₃]ClO₄·2H₂O (4). A 50 mg (0.065 mmol) portion of **1** was dissolved in a methanol/water mixture (2:4, 6 mL). AgClO₄ (44.5 mg, 0.22 mmol) was added, and the mixture was stirred for 1 h and then filtered from AgBr. To the filtrate was added 23.6 mg (0.143 mmol) of 7-MeG, and the mixture was heated to 50 °C under a slight N₂ pressure. The reaction was stopped after 3.5 h and cooled to room temperature, and then, methanol was allowed to evaporate slowly. After 3–4 days, X-ray quality crystals of **4** were obtained. Yield: 23 mg, 49%. Anal. Calcd: C% 25.1, N% 19.5, H% 2.2. Found: C% 25.1, N% 19.2, H% 2.4. ¹H NMR data (in D₂O, δ, ppm): H8 8.18, CH₃ 3.97. IR data (KBr pellet, ν, cm⁻¹): CO 2030 (s), 1908 (b), 1876 (b). MS data ESI+: 600.3 *m/z* = ([M]⁺ - H₂O).

[ReBr(7-MeG)₂(CO)₃]·2.5H₂O (5). To 30 mg (0.04 mmol) of **1** in a methanol/water mixture (2:1, 3 mL) was added 16.5 mg (0.1 mmol) of 7-MeG, and the mixture was heated to 50 °C under a slight N₂ pressure. After 3.5 h, the reaction was stopped, allowed to come to room temperature, concentrated, and purified on a short C18 column. A white crystalline solid was obtained. Yield: 18 mg, 68%. Anal. Calcd C% 26.5, N% 20.6, H% 2.1. Found: C% 26.2, N% 19.9, H% 2.2. ¹H NMR data (in D₂O, δ, ppm): H8 8.18, CH₃ 3.97. IR data (KBr pellet, ν, cm⁻¹): CO 2027 (s), 1897 (b). MS data ESI+: 600.3 *m/z* = ([M]⁺ - Br). Crystals suitable for X-ray diffraction were obtained by slow diffusion of pentane into a methanolic solution of the complex.

X-ray Crystallography. Suitable crystals were covered with Paratone N oil, mounted on top of a glass fiber, and immediately transferred to a Stoe IPDS diffractometer. Data were collected at 183(2) K using graphite-monochromated Mo Kα radiation (λ = 0.71073 Å). A total of 8000 reflections distributed over the whole limiting sphere were selected by the program SELECT and used for unit cell parameter refinement with the program CELL.¹² Data were corrected for Lorenz and polarization effects as well as for absorption (numerical). Structures were solved with direct method using SHELXS-97¹³ or SIR-97¹⁴ and were refined by full-matrix

least-squares methods on *F*² with SHELXL-97.¹⁵ CCDC files 223315–223318 contain the supplementary crystallographic data of complexes **2–5**. These data can be obtained free of charge via www.ccdc.cam.ac.uk/conts/retrieving.html. (They can also be obtained from the CCDC, 12 Union Road, Cambridge CB2 1EZ, U.K. Fax: +44 1223 336033. E-mail: deposit@ccdc.cam.ac.uk.)

Computational Details. Density functional theory (DFT) calculations carried out by use of the TURBOMOLE program package version 5.5,¹⁶ used the Vosko–Wilk–Nusair¹⁷ local density approximation (LDA) and the generalized gradient approximation (GGA) with corrections for exchange and correlation according to Becke¹⁸ and Perdew,¹⁹ respectively (BP86). The TURBOMOLE approach to DFT GGA calculations is based on the use of Gaussian-type-orbitals (GTO) as basis functions. Geometries were pre-optimized within the framework of the RI-*J* approximation²⁰ using accurate triple-ζ valence basis sets augmented by one polarization function TZV(P)^{20a} for Re, and slightly smaller polarized split-valence SV(P)^{20b} basis sets of double-ζ size for the remaining elements. In the final steps of the geometry optimizations, all elements were treated with the accurate TZV(P) basis sets. Linear transit (LT) calculations were performed to simulate the rotation of one coordinated purine ligand around the Re–N bond. For each fixed value of the reaction coordinate defined as the dihedral angle O_{H2O}–Re–N_{lig}–C_{lig}(H), all other structural parameters (degrees of freedom) were fully optimized.

Results

Synthetic Aspects. Reaction of **1** (in water [Re(H₂O)₃-(CO)₃]⁺) with 9-MeG or 7-MeG could be conveniently monitored by HPLC analysis. Both the mono- and bis-ligated species were observed, and in fact, reaction of the [Re(CO)₃]⁺ fragment with guanine bases led to the equilibrium depicted in Scheme 1. Although the reaction did not go to completion at a 1:2 stoichiometry, compounds **2–5** could be obtained as analytically pure, white microcrystalline solids when a slight excess of the corresponding base was utilized. We found no appreciable difference in the HPLC chromatograms if the reaction was carried out in water or a methanol/water mixture. Oriskovich had originally shown that the above-mentioned fragment can bind a single 9-ethylguanine (9-EtG) via the N7 atom after displacement of a labile CH₃CN to yield a stable complex, where the remaining two coordi-

- (13) Sheldrick, G. M. *Acta Crystallogr., Sect. A* **1990**, *46*, 467–473.
- (14) Altomare, A.; Burla, M. C.; Camalli, M.; Cascarano, G. L.; Giacovazzo, C.; Guagliardi, A.; Moliterni, A. G. G.; Polidori, G.; Spagna, R. *J. Appl. Crystallogr.* **1999**, *32*, 115–119.
- (15) Sheldrick, G. M. *SHELXL-97*; University of Göttingen: Göttingen, Germany, 1997.
- (16) *TURBOMOLE, Program package for ab initio electronic structure calculations*; Theoretical Chemistry, University of Karlsruhe: Germany, <http://www.turbomole.com>. (a) Ahlrichs, R.; Bär, M.; Häser, M.; Horn, H.; Kölmel, C. *Chem. Phys. Lett.* **1989**, *162*, 165–169. (b) Treutler, O.; Ahlrichs, R. *J. Chem. Phys.* **1995**, *102*, 346–354. (c) von Arnim, M.; Ahlrichs, R. *J. Comput. Chem.* **1998**, *19*, 1746–1757.
- (17) Vosko, S. H.; Wilk, L.; Nusair, M. *Can. J. Phys.* **1980**, *58*, 1200–1211.
- (18) Becke, A. D. *Phys. Rev. A* **1988**, *38*, 3098–3100.
- (19) (a) Perdew, J. P. *Phys. Rev. B* **1986**, *33*, 8822–8824. (b) Perdew, J. P. *Phys. Rev. B* **1986**, *34*, 7406. (c) Eichkorn, K.; Treutler, O.; Öhm, H.; Häser, M.; Ahlrichs, R. *Chem. Phys. Lett.* **1995**, *240*, 283–290. (d) Eichkorn, K.; Treutler, O.; Öhm, H.; Häser, M.; Ahlrichs, R. *Chem. Phys. Lett.* **1995**, *242*, 652. (e) Eichkorn, K.; Weigand, F.; Treutler, O.; Ahlrichs, R. *Theor. Chem. Acc.* **1997**, *97*, 119–124.
- (20) (a) Schäfer, A.; Huber, C.; Ahlrichs, R. *J. Chem. Phys.* **1994**, *100*, 5829–5835. (b) Schäfer, A.; Huber, C.; Ahlrichs, R. *J. Chem. Phys.* **1992**, *97*, 2571–2577.

(12) *CELL*, 2.92, 1999 ed.; STOE & Cie, GmbH: Darmstadt, Germany, 1999.

Scheme 1

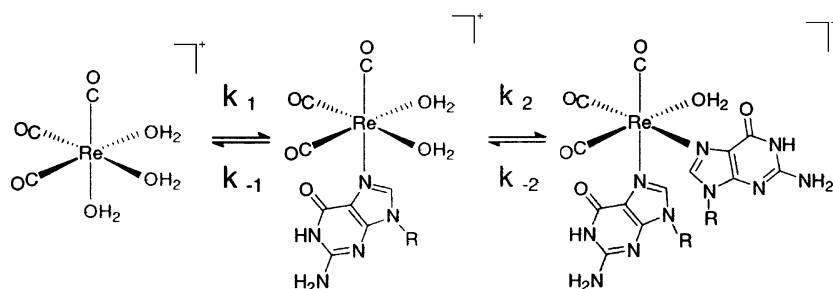


Table 1. Summary of X-ray Crystallographic Data

	2	3	4	5
formula	C ₁₅ H ₂₂ ClN ₁₀ O ₁₃ Re	C ₁₅ H ₁₈ BrN ₁₀ O ₇ Re	C ₁₆ H ₂₂ ClN ₁₀ O ₁₂ Re	C _{17.25} H _{21.5} BrN ₁₀ O ₆ Re
molecular mass	772.08	716.50	768.09	731.05
space group	<i>P</i> 2 ₁ / <i>n</i>	<i>P</i> 2 ₁ / <i>n</i>	<i>P</i> 2 ₁ / <i>c</i>	<i>P</i> 2 ₁ / <i>c</i>
<i>a</i> , Å	12.3307(10)	15.6260(13)	13.0708(9)	17.5117(9)
<i>b</i> , Å	16.2620(14)	9.5269(5)	15.4082(7)	9.8842(5)
<i>β</i> , deg	105.525(9)	76.951(10)	117.236(7)	100.824(7)
<i>c</i> , Å	13.7171(11)	15.4078(13)	14.3160(9)	15.3539(10)
<i>V</i> , Å ³	2650.2(4)	2234.5(3)	2563.5(3)	2610.3(3)
<i>Z</i>	4	4	4	4
<i>ρ</i> _{calcd} , g/cm ³	1.935	2.130	1.990	1.860
<i>R</i> ^{<i>a,b</i>}	0.0432	0.0715	0.0416	0.0640
w <i>R</i> ^{2<i>a,c</i>}	0.0984	0.1578	0.1016	0.1411
max, min peaks, e/Å ³	1.939, −2.185	1.831, −1.140	2.960, −2.214	1.188, −2.394

^a Observation criterion: $I > 2\sigma(I)$. ^b $R = \sum ||F_o| - |F_c|| / \sum |F_o|$. ^c $wR2 = \{\sum [w(F_o^2 - F_c^2)^2] / \sum [w(F_o^2)^2]\}^{1/2}$.

Table 2. Selected Bond Distances (Å) and Angles (deg) of Complexes 2–5^a

	2	3	4 ^b	5 ^b	Re(9-EtG) ^c
Distances					
Re–N(7)	2.203(4)	2.212(13)	2.213(3)	2.215(10)	2.220(10)
Re–N(17)	2.193(4)	2.186(13)	2.184(4)	2.198(10)	
Re–C(21)	1.922(7)	1.880(17)	1.931(4)	1.916(18)	1.875(17)
Re–C(22)	1.918(5)	1.916(15)	1.911(4)	1.891(15)	1.896(15)
Re–C(23)	1.959(6)	1.881(16)	1.893(4)	1.901(19)	1.919(14)
Re–O(1)	2.168(4)	2.167(11)	2.184(3)		
Re–Br(1)				2.599(2)	
Angles					
N(7)–Re–N(17)	83.05(16)	82.0(4)	86.46(13)	84.8(4)	
N(7)–Re–C(21)	96.7(2)	173.8(5)	178.08(15)	177.2(5)	176.1(6)
N(7)–Re–C(22)	92.4(2)	95.4(5)	92.78(16)	93.3(5)	93.8(5)
N(7)–Re–C(23)	172.3(2)	96.9(5)	92.76(16)	92.1(5)	97.8(5)
N(17)–Re–C(21)	91.6(2)	93.8(5)	92.37(17)	93.1(6)	
N(17)–Re–C(22)	175.0(2)	177.0(5)	176.91(16)	92.8(5)	
N(17)–Re–C(23)	97.5(2)	94.4(5)	92.15(17)	175.6(5)	
O(1)–Re–N(7)	83.30(17)	81.9(4)	85.95(12)		
O(1)–Re–N(17)	81.64(16)	88.0(4)	84.04(13)		
Br(1)–Re–N(7)				83.3(3)	
Br(1)–Re–N(17)				84.5(3)	
C(21)–Re–C(22)	86.8(3)	88.7(6)	88.3(2)	88.6(6)	87.0(7)
C(21)–Re–C(23)	91.0(3)	87.9(6)	88.8(2)	89.9(6)	87.3(7)
C(22)–Re–C(23)	87.3(2)	87.5(6)	90.9(2)	90.5(6)	89.4(6)

^a C(21), C(22), C(23) refer to carbonyl groups. ^b For complexes 4 and 5, N(7) and N(17) refer to N(9) and N(19), respectively, that is, to the N atoms bound to Re. ^c See ref 21.

nation sites were occupied by bipyridine.²¹ In this case, coordination of purine ligands occurred via displacement of the weakly bound water and/or methanol molecules.

X-ray Crystallography. Crystal data and experiment details are listed in Table 1 while selected geometrical parameters are listed in Table 2. Crystals suitable for X-ray analysis were obtained in one of two ways. Slow solvent evaporation of a methanol/water solution gave crystals of

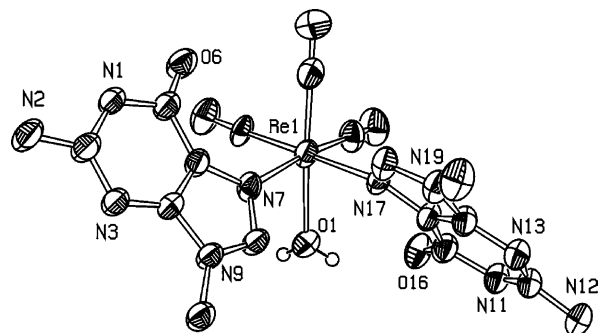


Figure 1. ORTEP view of [Re(9-MeG)₂(H₂O)(CO)₃]⁺ (cation of 2) with 50% probability thermal ellipsoids.

complexes 3 and 4, while vapor diffusion of pentane into a methanolic solution gave crystals of 2 and 5. In all but one case, a water molecule is found occupying the sixth coordination site with exception of 5, where a bromide is found. All relevant bonds and angles (Table 2) are in good agreement with the structure reported by Oriskovich et al.²¹ An ORTEP view of the cation of 2 is given in Figure 1. In this complex the two 9-MeG bases are in HT orientation with one base stabilized by a hydrogen bond between the carbonyl oxygen (O(16) in Figure 1) and a proton of the coordinated H₂O molecule. In complex 3 (see Figure 2), the same bases are found in an HH orientation. Both carbonyl oxygens can now participate in hydrogen bonding with the coordinated water molecule; however, only O(6) shows a significant interaction (coordinated water–H–O(6) bond = 1.88(8) Å; coordinated water–H–O(16) bond = 3.07(9) Å, see Figure 2). It is also interesting to note that in crystal structures of *cis*-[(NH₃)₂Pt(9-EtG)₂](X)₂ (X = Cl[−], ¹/₂SO₄^{2−} or ¹/₂Pt(CN)₄^{2−}) where the two bases are found in a HH conformation, only a single intramolecular hydrogen bond is formed between O(6) and a NH₃ group.²²

(21) Oriskovich, T. A.; White, P. S.; Thorp, H. H. *Inorg. Chem.* **1995**, *34*, 1629–1631.

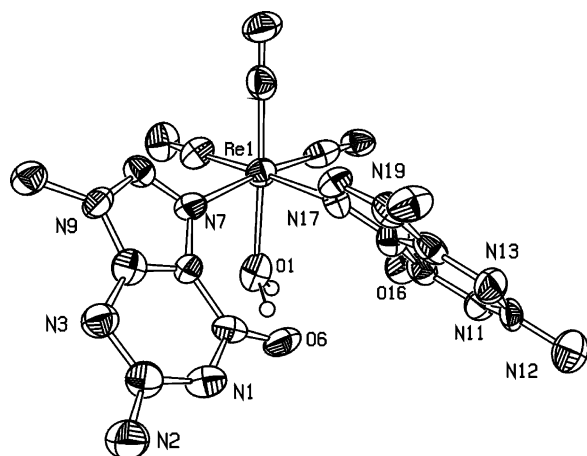


Figure 2. ORTEP view of $[\text{Re}(9\text{-MeG})_2(\text{H}_2\text{O})(\text{CO})_3]^+$ (cation of **3**) with 50% probability thermal ellipsoids.

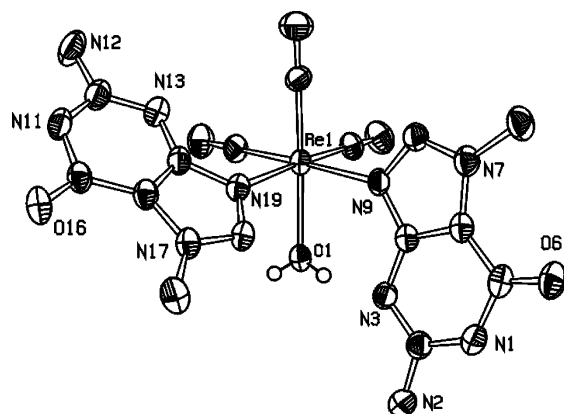


Figure 3. ORTEP view of $[\text{Re}(7\text{-MeG})_2(\text{H}_2\text{O})(\text{CO})_3]^+$ (cation of **4**) with 50% probability thermal ellipsoids.

Complexes with 7-MeG also exhibit both HH and HT orientation of the bases. An ORTEP view of the cation of **4** is given in Figure 3. The structural features of this complex resemble those of **2**. In this case the two purines are in an HT orientation with one base stabilized by a hydrogen bond between N(3) and the a proton of the coordinated H_2O molecule (coordinated water-H-N(3) bond = 1.93(7) Å, see Figure 3). Complex **5** is the only complex bearing a bromide at the sixth coordination site. An ORTEP view of this molecule is given in Figure 4. Interestingly, the two bases were found in a HH orientation.

NMR Studies. ^1H NMR spectra of **2–5** are easily interpreted since in D_2O only two resonances are found, one in the aromatic region, while the other is in the 3–4 ppm region, with a relative intensity of 1:3. These signals correspond to the aromatic H(8) proton and to the methyl group covalently bound to the N(9) or N(7) atom. Figure 5 shows the aromatic region of ^1H NMR spectra obtained when crystals of **2** and of **3** are dissolved in D_2O . The single major peak resonating at 8.09 ppm corresponds to the bis-ligated species (i.e., **2** or **3**), while the two smaller signals flanking it, at 8.33 and 7.81 ppm, correspond to the mono-ligated species and to free 9-MeG, respectively. With time, the

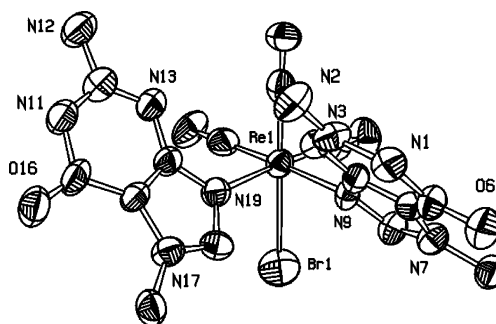


Figure 4. ORTEP view of $[\text{ReBr}(7\text{-MeG})_2(\text{CO})_3]$ (**5**) with 50% probability thermal ellipsoids.

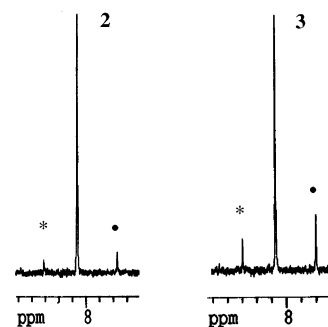


Figure 5. ^1H NMR spectrum (7.7–8.5 ppm) of crystals of **2** (left) and **3** in D_2O (298 K). The asterisk (*) indicates the mono-bound species; the filled circle (●) indicates free 9-MeG.

intensity of the small signals increases while the signal of **2** (and/or **3**) decreases, correspondingly, until the equilibrium depicted in Scheme 1 is reached. When crystals of **4** and **5** are dissolved in D_2O , a similar spectrum and a similar behavior is observed.

Raman Spectroscopy. Raman spectra of crystals of **2** and **3** and of 9-MeG are shown in Figure 8. The spectra were recorded and compared in order to see if the intermolecular base stacking observed in the solid state structure of **3** (Figure 9B) would give rise to a Raman hypochromic effect.²³ All spectra show highly characteristic guanine vibrational modes around 1580, 1500, and 1370 cm^{-1} . In addition, spectra of **2** and **3** show characteristic carbonyl ligand bands around 2030–1890 cm^{-1} . We find no appreciable decrease in signal intensity of the guanine bands in the spectrum of **3**. In this latter spectrum, the bands at around 1580 and 1370 cm^{-1} are actually found to have a higher relative intensity to the carbonyl ligand bands when compared to the spectrum of **2**. The spectra we report bear a resemblance to those of HH conformers of 9-EtG adducts of cisplatin.²² As in this latter case, it is likely that since the intermolecular base stacking does not exceed the dimer level in **3**, it cannot cause a large enough hypochromic effect to reduce the intensity of the guanine bands.

Discussion

Crystal Packing. Packing diagrams of the four structures are given in Figure 9. Complex **2** (Figure 9A) shows

(22) Schöllhorn, H.; Raudaschl-Sieber, G.; Müller, G.; Thewalt, U.; Lippert, B. *J. Am. Chem. Soc.* **1985**, *107*, 5932–5937.

(23) (a) Tomlinson, B. L.; Peticolas, W. L. *J. Chem. Phys.* **1970**, *52*, 2154–2156. (b) Tinoco, I., Jr. *J. Am. Chem. Soc.* **1960**, *82*, 4785–4790. (c) Rhodes, W. *J. Am. Chem. Soc.* **1961**, *83*, 3609–3617.

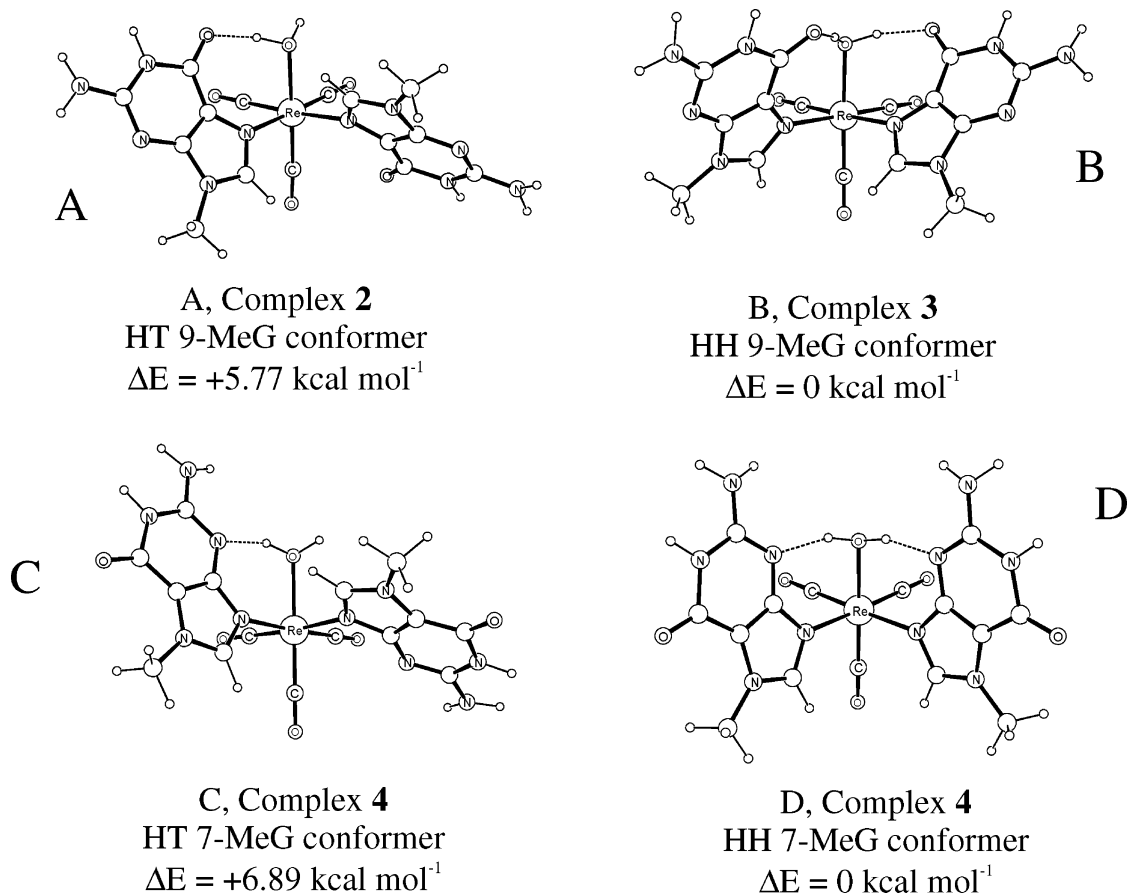


Figure 6. Optimized geometries and relative energies (ΔE) of HH and HT conformers of complexes 2–4 (A–D).

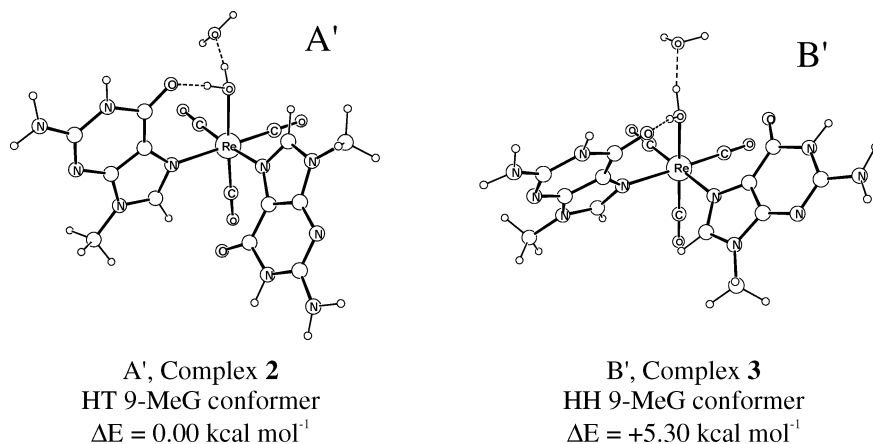


Figure 7. Optimized geometries and relative energies (ΔE) of complexes 2·H₂O (A') and 3·H₂O (B').

alternating metal complexes separated along the *x*-axis by the perchlorate counterions (on average Re–Cl > 6 Å). The packing is stabilized by extensive hydrogen bonding interactions involving the complex, the counterion and the water molecules (see Hydrogen Bonding subsection). We find no evidence of base–base π -stacking interactions in this case. Complex 3 (Figure 9B) shows π -stacking of one coordinated purine involving the six member ring of the bases which are separated on average by 3.8 Å. The bases participating in π -stacking are oriented in an antiparallel fashion. In complex 4 (Figure 9C) both bases participate in π -stacking interactions; however, one couple of bases shows only partial overlap. The other two bases are fully eclipsed and are

oriented in an antiparallel fashion so as to maximize dipole–dipole interactions. In this latter case the mean average base–base separation is 3.8 Å. The packing diagram of complex 5 (Figure 9D) shows two cavities along the (001) projection. The larger of the two cavities is occupied by disordered pentane molecules while the smaller one is occupied by water molecules. Solvent molecules are, however, not shown in Figure 9D for clarity. We find no evidence of base–base π -stacking interactions, and the overlap involving the six member ring visible in the figure is only apparent as the rings are separated by a distance greater than 7.5 Å.

Base Geometry and Conformation. Extensive studies on *cis*-PtA₂{d(GpG)} and simpler *cis*-PtA₂G₂ adducts have now

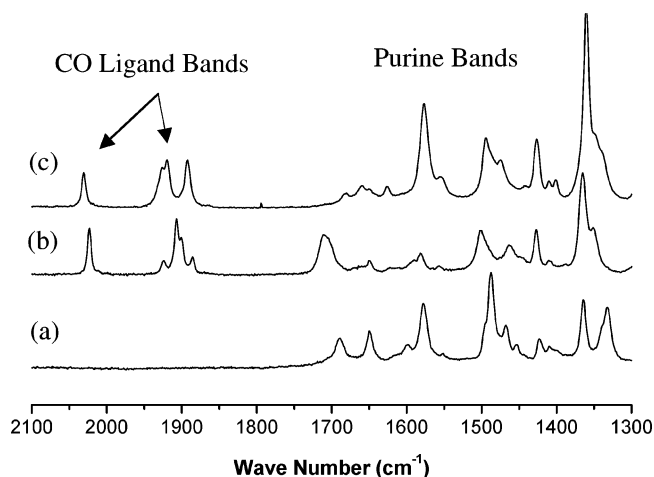


Figure 8. Solid state Raman spectra (2100–1300 cm^{-1}) of 9-MeG (a), 2 (b), and 3 (c).

established that the two bases can assume an HH and an HT conformation around the metal core.^{24–35} Solid state structural data indicate that base tilt (or cant) can have two different directions, right-handed (R) and left-handed (L).^{24,31–35} Furthermore, HT isomers can be divided into two groups differing in the degree of canting. ΔHTR and ΔTHL isomers show less tilted bases while ΛHTR and ΔTHL isomers show more tilted bases.^{5b–c,36–38} In discussing the Re structures we present in this study, we use the same nomenclature used to describe the HT and HH isomers of Pt compounds.

In all Re structures, the two bases show right-hand canting. The two HT isomers of 7- and 9-MeG are of ΛHTR subgroup. This form has, to our knowledge, never been observed in the solid state structure of a metal fragment bound to two nucleotides. For *cis*-PtA₂G₂ models where G = nucleoside and nucleotide, for example, the ΔHTR form is observed exclusively in the solid state.^{25–28,39} A high degree of canting allowing the ΛHTR form is found only when G

is not a 5'-nucleotide or when the base is part of an oligonucleotide.^{22,29,31–34,40–41} Therefore, structures 2 and 4 represent the first examples of ΔHTR forms of a metal fragment bound to two nucleotides. The ΔHTR form is unfavored by electronic (dipole–dipole) interactions. It is now established that G(dipole)–G(dipole) interactions favor the less tilted HT atropisomer as this orientation of the bases places the H(8) end of the dipole closer to the negative six-member ring of the *cis*-G base than in the more tilted form.^{3,5,36–38} This feature stabilizes the ΔHTR form, and it is one of the reasons for the exclusive crystallization of this form when the two bases are nucleotides. In structures 2 and 4, this is not the case, and the ΛHTR form is observed.

Dihedral Angles. The base–base (B/B') and the base–coordination plane (B/CP) dihedral angles are useful parameters for comparing structural features of metal complexes of purines. B/B' is the angle formed by the intersection of the planes that pass through the two bases in a *cis* arrangement while B/CP is the angle formed by the intersection of the plane that passes through one of the bases and the plane defined by Re, the two N atoms of the bases coordinated to it and two C atoms *trans* to them. The B/B' angle is calculated according to the method outlined by Orbell, Marzilli, and Kistenmacher by confining one of the two bases to the plane of the paper so that the N → Re vector points leftward and the second base projects outward toward the viewer.⁴² Relevant conformational parameters and dihedral angles are given in Table 3.

The average B/B' angle of the Re complexes is 65° smaller than the average B/B' angle reported for *cis*-bis nucleotide complexes of Pt where the angle is generally greater than 70°. ^{22,25,30,39} B/CP angles are small (near 50°) for all complexes except 4 where one of the bases shows a rather large B/CP angle of 78° while the other base a very small angle of 38°. Orbell et al. found that it was possible in some cases to rationalize a large (near 90°) or a small B/CP dihedral angle in terms of intramolecular effects. They found, for example, that interligand hydrogen bonding tends to favor a small B/CP angle, while repulsive interligand steric factors tend to favor a large B/CP angle.⁴⁰ All Re complexes, with the exception of 5, show a strong (on average 1.91 ± 0.03 Å) intramolecular hydrogen bond between one base and the coordinated water molecule and show no intramolecular hydrogen bonding between coordinated purines. Complex 4, however, is the only complex in which both bases participate in π -stacking interactions, and neither of them shows base–base intermolecular hydrogen bonding. In this case, therefore, intermolecular rather than intramolecular effects can rationalize the B/CP angles. Intermolecular base–base hydrogen bonding tends to favor a small B/CP angle, while π -stacking interactions tend to favor a large B/CP angle.

- (24) Kozelka, J.; Fouchet, M.-H.; Chottard, J.-C. *Eur. J. Biochem.* **1992**, *205*, 895–906.
- (25) Cramer, R. E.; Dahlstrom, P. L.; Seu, M. J. T.; Norton, T.; Kashiwagi, M. *Inorg. Chem.* **1980**, *19*, 148–154.
- (26) Marzilli, L. G.; Chalilpoyil, P.; Chiang, C. C.; Kistenmacher, T. J. *J. Am. Chem. Soc.* **1980**, *102*, 2480–2482.
- (27) Kistenmacher, T. J.; Chiang, C. C.; Chalilpoyil, P.; Marzilli, L. G. *J. Am. Chem. Soc.* **1979**, *101*, 1143–1148.
- (28) Barnham, K. J.; Bauer, C. J.; Djuran, M. I.; Mazid, M. A.; Rau, T.; Sadler, P. J. *Inorg. Chem.* **1995**, *34*, 2826–2832.
- (29) Lippert, B.; Raudaschl, G.; Lock, C. J. L.; Pilon, P. *Inorg. Chim. Acta* **1984**, *93*, 43–50.
- (30) Longato, B.; Bandoli, G.; Trovò, G.; Marasciulo, E.; Valle, G. *Inorg. Chem.* **1995**, *34*, 1745–1750.
- (31) Grabner, S.; Plavec, J.; Bukovec, N.; Di Leo, D.; Cini, R.; Natile, G.; *J. Chem. Soc., Dalton Trans.* **1998**, *9*, 1447–1451.
- (32) Cini, R.; Grabner, S.; Bukovec, N.; Cesarino, L.; Natile, G. *Eur. J. Inorg. Chem.* **1999**, *7*, 1601–1607.
- (33) Sindellari, L.; Schöllhorn, H.; Thewalt, U.; Raudaschl-Sieber, G.; Lippert, B. *Inorg. Chim. Acta* **1990**, *168*, 27–32.
- (34) Sinur, A.; Grabner, S. *Acta Crystallogr., Sect. C* **1995**, *51*, 1769–1772.
- (35) Grehl, M.; Krebs, B. *Inorg. Chem.* **1994**, *33*, 3877–3885.
- (36) Marzilli, L. G.; Intini, F. P.; Kiser, D.; Wong, H. C.; Ano, S. O.; Marzilli, P. A.; Natile, G. *Inorg. Chem.* **1998**, *37*, 6898–6905.
- (37) Ano, S. O.; Intini, F. P.; Natile, G.; Marzilli, L. G. *Inorg. Chem.* **1999**, *38*, 2989–2999.
- (38) Saad, J. S.; Scarica, T.; Shinozuka, K.; Natile, G.; Marzilli, L. G. *Inorg. Chem.* **2002**, *41*, 546–557.
- (39) Gellert, R. W.; Bau, R. *J. Am. Chem. Soc.* **1975**, *97*, 7379–7380.

- (40) Orbell, J. D.; Wilkowski, K.; De Castro, B.; Marzilli, L. G.; Kistenmacher, T. J. *Inorg. Chem.* **1982**, *21*, 813–821.
- (41) Admiraal, G.; Van der Veer, J. L.; De Graaff, R. A. G.; Den Hartog, J. H. J.; Reedijk, J. *J. Am. Chem. Soc.* **1987**, *109*, 592–594.
- (42) Orbell, J. D.; Marzilli, L. G.; Kistenmacher, T. J. *J. Am. Chem. Soc.* **1981**, *103*, 5126–5133.

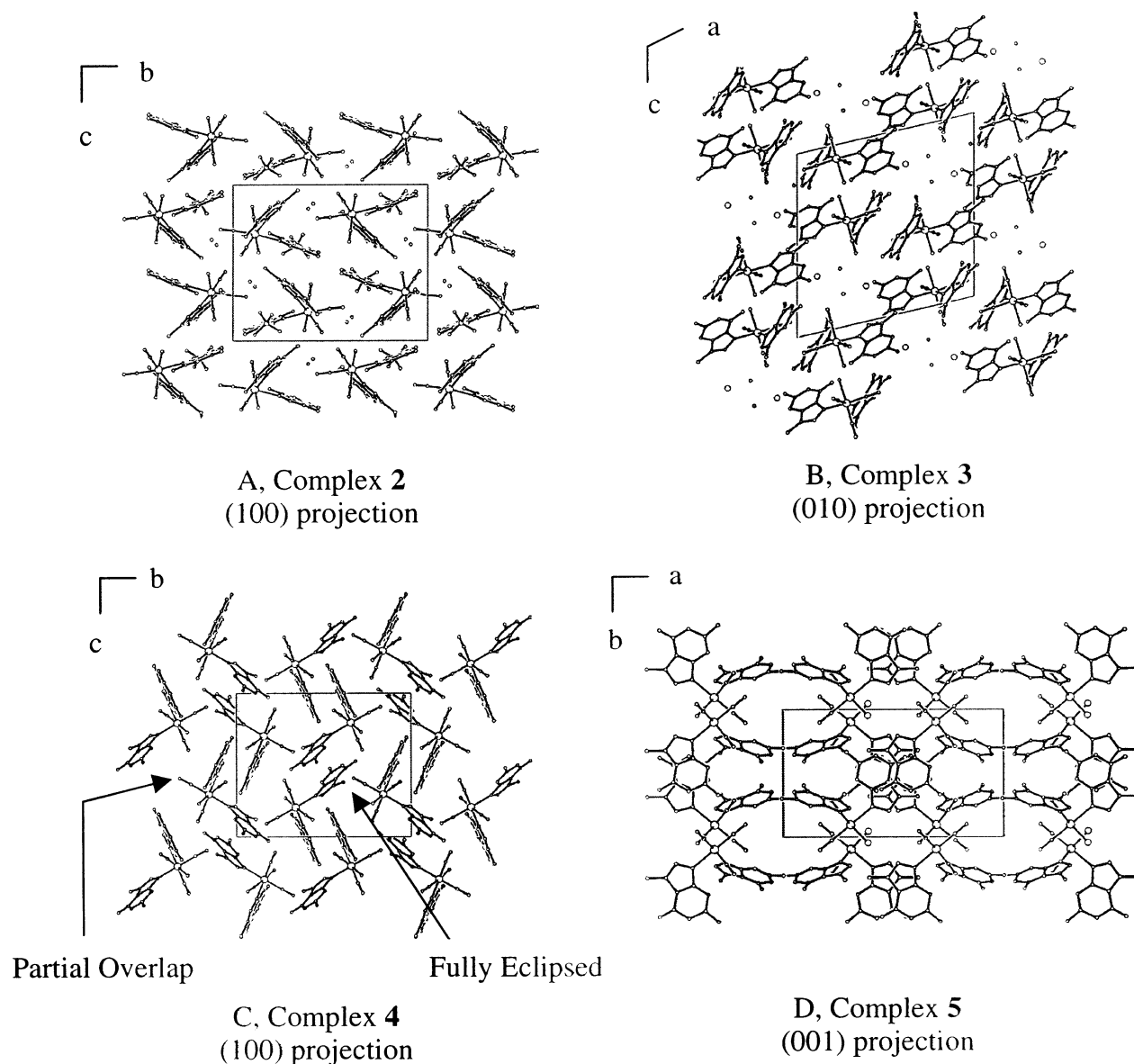


Figure 9. Perspective views of the crystal packing of structures **2–5** (A–D) generated by PLUTON.⁴⁴ Solvent molecules and counterion are not shown in C and D for clarity.

Table 3. Conformational Parameters of Complexes **2–5**

	dihedral angles ^a (deg)			L N _B –Re–N _{B'}	
	B/B'	B/CP	B'/CP	(deg)	base canting
X-ray Structure					
2	66	48	50	83.06(17)	ΔHTR
3	57	51	46	81.9(4)	HHR
4	75	38	78	86.45(13)	ΔHTR
5	62	48	47	84.8(4)	HHR
Optimized Geometry					
A	84	51	61	86.4	
B	86	64	53	89.1	
C	84	30	79	86.3	
D	81	71	86	87.4	

^a See text for definitions.

Hydrogen Bonding. All structures have extensive hydrogen-bonding interactions between the guanines and the counterions and the water molecules present in the crystals. Complete tables of these interactions are given in Supporting Information. Solvent molecule–guanine hydrogen-bonding

involves mainly the N(2)H₂ and O(6) groups of the bases. Although the Re complexes are generally well separated (on average in the four structures Re–Re > 8 Å), some intercomplex interactions occur. All structures, with the exception of **4**, shows base–base intermolecular hydrogen bonding. These interactions are shown in Figure 10. Complex **2** (Figure 10A) shows the unusual base-pairing scheme involving N(2) and N(3) (N(2)H–N(3) bond 2.16(4) Å) which has been observed previously in the HT structure of the Pt–acyclovir complex.³¹ The intermolecular base–base hydrogen bonding scheme of complex **3** (Figure 10B) involves, on the other hand, the carbonyl O(6) atom and N(2)H₂ and N(1)H with distances of 2.34(2) and 1.95(2) Å, respectively. To our knowledge, this type of intermolecular interaction has never been reported in *cis*-bis purine metal complexes. Complex **5** shows the most unusual intermolecular base–base hydrogen bonding pair of the three structures. The hydrogen bonding scheme of complex **5**

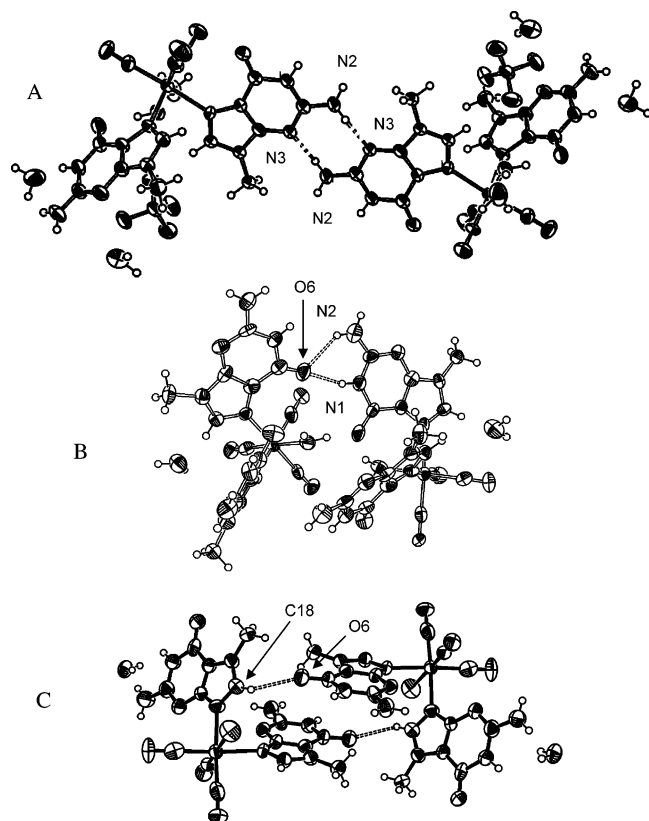


Figure 10. Intermolecular base–base hydrogen bonding in complexes **2** (A), **3** (B), and **5** (C).

(Figure 10C) involves the carbonyl O(6) atom and the H(8) proton (2.44(1) Å). This type of interaction can be explained in electronic terms. As it is the case with other metals, the binding by N(7) to Re(I) leads to donation of electron density from the base imidazole ring to the metal. This interaction makes the H(8) proton, already electron deficient and bearing a partial positive charge,⁴³ even more positive and therefore likely to participate in hydrogen bonding.

Theoretical Calculations. In order to obtain further information about the relative orientation of the coordinated purine ligands, the minima of the total energy surface corresponding to both HH and HT conformations of complexes $[\text{Re}(\text{9-MeG})_2(\text{H}_2\text{O})(\text{CO}_3)]^+$ and $[\text{Re}(\text{7-MeG})_2(\text{H}_2\text{O})(\text{CO}_3)]^+$ have been first fully optimized by aid of DFT calculations.¹⁶ The most stable conformations found for both complexes exhibit a HH orientation while the HT conformers lie +5.8 and +6.9 kcal/mol higher in energy for complexes with 9-MeG and 7-MeG, respectively (Figure 6). The calculated values for the base–base (B/B') and the base–coordination plane (B/CP) dihedral angles defining the orientations of the purine ligands in the optimized conformers are in a reasonable agreement with those observed in the corresponding crystal structures (Table 3). However, it is well established that, in the gas phase (DFT calculations level), the lowest energy structure maximizes the hydrogen bonding between ligands whereas in condensed phase systems, the hydrogen bonding will most likely be with

surrounding solvent molecules. Thus, we can assume that the calculated energetic preference for the HH conformers is due to the fact that the two ligands in an HH orientation are well suited to make two intramolecular hydrogen bonds with the coordinated water, whereas the bases in an HT orientation can support only one such interaction. Consequently, we performed further calculations in which a free water molecule was added in the vicinity of the coordinated water molecule, in order to allow only one guanine ligand to interact with the coordinated water in both conformers. The most stable conformations found for both complexes now exhibit HT orientations: the HH conformers are higher in energy by +5.3 and +4.2 kcal/mol for complexes with 9-MeG and 7-MeG, respectively (see Figure 7 and Supporting Information for further details). Furthermore, linear transit calculations simulating the rotation of one ligand around the Re–N bond in both cases of the *cis*-bis-guanine complex with 9-MeG and 7-MeG show that the energetic barriers ΔE rise approximately to 8.7 and 6.5 kcal/mol, respectively (the noncoordinated water molecule being still involved in the calculation). Finally, from our DFT calculations, we can conclude that in solution free rotation of the guanine ligands occurs, leading to relative orientations of the ligands in the solid state mainly governed by intra- or intermolecular interactions.

Conclusions

Our results show that guanine ligands can assume both an HH and an HT conformation in an octahedral complex around the Re^{I} tricarbonyl core. The structural evidence we have presented clearly shows the two conformations. Although it is clear that intermolecular packing forces are responsible for the exclusive crystallization of one form, the ^1H NMR evidence indicates that these two forms are present in solution in equilibrium. Because conformer interconversion is fast on the NMR time scale, it is impossible to use NMR methods to distinguish among the forms present in solution. This is the same “dynamic motion problem” present in most cisplatin adducts of untethered guanines.^{3, 5}

The presence of a single H(8) resonance in the ^1H NMR spectrum of **2** and **3** indicates that the two guanines can freely rotate about the Re–N7(9) bond. This implies that no steric hindrance is imposed by the O(6) carbonyl oxygen. The presence of HH and HT conformers in complexes with either 9-MeG or 7-MeG in the solid state and in solution delineates the fact that intramolecular hydrogen bonding and steric hindrance imposed by the carbonyl oxygen of coordinated guanines are not driving forces for the preference of one or the other conformation. DFT calculations confirmed the expected free rotation of the guanine ligands in solution leading to relative orientations of the ligands, because of small energy differences between conformers and relatively low energetic barriers leading from one conformer to the other.

An important implication arises from these studies. As mentioned in the Introduction, this study is presented within a contest that focuses on the interaction of cisplatin adducts with DNA bases, and in particular guanine. If the hypothesis

(43) Marzilli, L. G.; Marzilli, P. A.; Alessio, E. *Pure Appl. Chem.* **1998**, *70*, 961–968.

(44) Spek, A. L. *Acta Crystallogr., Sect. A* **1990**, *46*, 34.

advanced by Lippard to explain the activity of the drug is correct, new metal-based chemotoxic agents that are intended to act at the DNA level in a fashion similar to cisplatin should show accessibility to an HH conformer. We have shown that the $[\text{Re}(\text{H}_2\text{O})_3(\text{CO})_3]^+$ complex can be utilized as a DNA-targeting metal fragment of octahedral geometry. Finally, the results we have presented tentatively suggest that the mechanism of cytotoxicity exhibited by certain rhenium compounds might parallel that of cisplatin.

Acknowledgment. We thank Professor Richard H. Fish (University of California, Berkeley) for helpful discussion and useful insights, and Mallinckrodt Med. Inc Petten NL, for financial support.

Supporting Information Available: Details of theoretical calculations and tables of hydrogen bonds for structures **2–5**. This material is available free of charge via the Internet at <http://pubs.acs.org>.

IC035012A